

# Contribution of grain boundary sliding in low-temperature superplasticity of ultrafine-grained aluminum alloys

F.C. Liu and Z.Y. Ma\*

*Shenyang National Laboratory for Materials Science, Institute of Metal Research, Chinese Academy of Sciences, 72 Wenhua Road, Shenyang 110016, China*

Received 10 September 2009; revised 4 October 2009; accepted 7 October 2009  
Available online 13 October 2009

Ultrafine-grained (0.6  $\mu\text{m}$ ) Al–Mg–Sc alloy with predominant high-angle boundaries was produced by friction stir processing. A superplastic elongation of 210% was obtained at 175  $^{\circ}\text{C}$ , and the optimum strain rate and maximum elongation increased with increasing temperature. Marker lines were scratched on the polished specimen surfaces using a nano-indenter to measure grain boundary sliding (GBS) offsets during deformation, which indicated that the GBS contribution to the strain exceeded 50% at 175  $^{\circ}\text{C}$  and increased with increases in strain and temperature.

© 2009 Acta Materialia Inc. Published by Elsevier Ltd. All rights reserved.

**Keywords:** Superplasticity; Friction stir processing; Ultrafine-grained structure; Aluminum alloys; Friction stir welding

Superplastic forming (SPF) at higher strain rates or lower temperatures is highly desirable in industrial fabrication. There are obvious advantages in conducting SPF at a lower temperature. For example, a lower forming temperature would save energy, improve the surface quality of the formed component, prevent severe grain growth and reduce the level of cavitation and solute loss from the surface layer, thus maintaining better post-forming properties [1].

In the past few years, many efforts have been made to produce ultrafine-grained (UFG) aluminum alloys suitable for low-temperature superplasticity (LTSP), as summarized in Table 1 [2–23], by various severe plastic deformation techniques, such as thermo-mechanical treatment/processing (TMT/TMP) [12,20,21,23], equal channel angular pressing (ECAP) [6,7,9–11,14,18,19], high-pressure torsion (HPT) [13,22], multi-axial alternative forging (MAF) [8], accumulative roll bonding (ARB) [15] and friction stir processing (FSP) [2–5]. Among these techniques, FSP, a novel processing technique developed based on the basic principles of friction stir welding (FSW) [24,25], is especially attractive owing to its simplicity, effectiveness and variability for microstructure modification.

In spite of a great number of reports about LTSP of aluminum alloys, the LTSP deformation mechanism of

UFG aluminum alloys is not well understood. Table 1 shows that the strain rate sensitivity for LTSP is generally between 0.3 and 0.4, lower than the characteristic sensitivity for grain boundary sliding (GBS), which is 0.5. Pu et al. [20] suggested that viscous dislocation creep would control the LTSP flow of 8090Al alloy. However, Park et al. [10] claimed that the LTSP of the ECAP UFG 5083Al was attributed to GBS, which was rate controlled by grain boundary diffusion. Hsiao and Huang [12] observed that GBS did occur in TMT 5083Al at temperatures as low as 200  $^{\circ}\text{C}$ . During the initial LTSP stage, the primary deformation mechanisms were solute drag creep plus minor power-law creep. At later stages, GBS gradually controlled the deformation [12]. It seems that there is no consensus on the deformation mechanism of LTSP.

Measuring the offsets of marker lines on the surfaces of deformed specimens is a direct and effective approach to estimating the contribution of GBS to the total strain [26,27]. For micron-grained alloys, the marker lines were usually scratched on the tensile specimen surface by a lens paper which was pasted with a small amount of 3- $\mu\text{m}$  diamond powders [26–29]. However, aluminum alloys exhibiting LTSP generally had a submicron grain size (Table 1). Obviously, the marker lines scratched using 3- $\mu\text{m}$  diamond powders were oversized for UFG.

In this study, a novel method of scratching nano-sized marker lines using a nano-indenter is presented. The advantages of this method are obvious. First, the marker lines can be scratched exactly parallel to the

\* Corresponding author. Tel./fax: +86 24 83978908; e-mail: [zyrna@imr.ac.cn](mailto:zyrna@imr.ac.cn)

**Table 1.** Summary of representative LTSP reports in aluminum alloys.

Alloy	Processing	Grain size ( $\mu\text{m}$ )	Elongation (%)	Temperature ( $^{\circ}\text{C}$ )	Strain rate ( $\text{s}^{-1}$ )	$m$ value	Year [Reference]
Al–Mg–Sc	FSP	0.7	235	200	$1 \times 10^{-4}$	0.33	2008 [2]
7075Al	FSP	0.8	350	200	$1 \times 10^{-5}$	0.36	2007 [3]
Al–4Mg–1Zr	FSP	0.7	240	175	$1 \times 10^{-4}$	0.34	2005 [4]
Al–Zn–Mg–Sc	FSP	0.68	525	220	$1 \times 10^{-2}$	0.33	2005 [5]
1570Al	ECAP	$\sim 1.0$	$\sim 1110$	350	$1.4 \times 10^{-2}$	0.39	2004 [6]
5083Al	ECAP	$\sim 0.3$	315	275	$5 \times 10^{-4}$	0.4	2004 [7]
5083Al	MAF	$\sim 0.8$	340	200	$2.8 \times 10^{-3}$	0.39	2003 [8]
7055Al	ECAP	$\sim 1$	320	300	$5.6 \times 10^{-5}$	0.34	2003 [9]
5083Al	ECAP	0.3	250	250	$5 \times 10^{-4}$	0.4	2002 [10]
Al–3Mg–0.2Sc	ECAP	0.2	420	200	$3 \times 10^{-4}$	–	2002 [11]
5083Al	TMP	$\sim 0.5$	511	230	$2 \times 10^{-3}$	$\sim 0.35$	2002 [12]
1420Al	HPT	$\sim 0.1$	330	250	$1 \times 10^{-1}$	0.29	2001 [13]
Al–3Mg–0.2Sc	ECAP	0.2	1280	300	$1 \times 10^{-2}$	$\sim 0.5$	2001 [14]
5083Al	ARB	0.28	230	200	$1.7 \times 10^{-3}$	0.37	1999 [15]
5083Al	Rolling	$\sim 0.5$	400	250	$1 \times 10^{-3}$	0.3–0.4	1998 [16]
Al–5.5Mg	Rolling	30–450	228	300	$1 \times 10^{-4}$	0.29	1998 [17]
1420Al	ECAP	1.2	$\sim 620$	250	$1 \times 10^{-3}$	–	1998 [18]
2004Al	ECAP	$\sim 0.5$	970	300	$1 \times 10^{-2}$	–	1997 [19]
Al–Mg–Li–Zr	ECAP	1.2	1180	350	$1 \times 10^{-2}$	–	1997 [19]
8090Al	TMP	0.7	710	350	$8 \times 10^{-4}$	$\sim 0.37$	1995 [20]
Al–10Mg–0.1Zr	TMP		1100	300	$1 \times 10^{-3}$	$\sim 0.5$	1993 [21]
Al–4Cu–0.5Zr	HPT	0.3	250	220	$3 \times 10^{-4}$		1993 [22]
Al–10Mg–0.5Mn	TMT		400	300	$1 \times 10^{-3}$		1986 [23]

tensile direction. Second, the offsets of the nano-sized marker lines on the UFG materials after deformation are easily measured. Thus, it is possible to estimate quantitatively the contribution of GBS to the total strain at low temperature.

It has been reported that FSP aluminum alloys with predominant high angle grain boundaries (HAGB) exhibited good LTSP [2–5]. In particular, UFG FSP Al–4Mg–1Zr exhibited LTSP at 175  $^{\circ}\text{C}$  [4]. This is the first report on the LTSP of aluminum alloys  $< 0.5 T_m$ , where  $T_m$  is the melting temperature of aluminum expressed in kelvins. Thus, it would be interesting to find out whether the LTSP of UFG FSP aluminum alloys is associated with predominant HAGB, and whether GBS is the primary deformation mechanism for LTSP. In this work, the GBS contribution to LTSP of a UFG FSP Al–Mg–Sc alloy was examined by measuring the offsets of marker lines scratched by the nano-indenter. The aim is to elucidate the deformation mechanism of the UFG aluminum alloys at temperatures as low as 175  $^{\circ}\text{C}$ .

A  $300 \times 70 \times 8\text{-mm}$  ( $L \times W \times H$ ) extruded plate with composition Al–5.33 Mg–0.23Sc–0.49Mn–0.14Fe–0.06Zr (in wt.%) was used in this study. A single-pass FSP was carried out on the extruded plate at a tool rotation rate of 400 rpm and a traverse speed of  $25 \text{ mm min}^{-1}$ , with room-temperature water quenching the plate immediately. A steel tool with a concave shoulder 14 mm in diameter and a threaded conical pin with root diameter 5 mm, tip diameter 3.5 mm and length 4.5 mm was used. Microstructural characterization was performed on the cross section of the stir zone (SZ) transverse to the FSP direction with scanning electron microscopy (SEM). The samples for SEM were lightly electropolished to produce a strain-free surface. Electron backscatter diffraction (EBSD) orientation maps were obtained using a ZEISS SUPRA 35, operated at 20 kV, and interfaced with an HKL Channel EBSD system. Kikuchi patterns were obtained automatically at a step

of 0.05  $\mu\text{m}$  using a small beam spot size. Owing to the limited angular resolution, misorientations  $< 2^{\circ}$  were not considered.

Dog-bone-shaped superplastic tensile specimens (2.5 mm gage length, 1.4 mm gage width and 1.0 mm gage thickness) were electro-discharge machined from the SZ of the FSP sample transverse to the FSP direction. These samples were subsequently ground and polished to a final thickness of  $\sim 0.8$  mm. Constant crosshead speed tensile tests were conducted using an INSTRON 5848 micro-tester. For the specimens used to investigate the contribution of GBS, the surfaces of the tensile specimens were polished to a mirror-like finish. Three parallel marker lines were scratched on the polished surfaces parallel to the tensile axis, using a MTS nano-indenter XP. These specimens were pulled to an elongation of 20, 40 and 80%, respectively, at different temperatures. The sliding offsets perpendicular to the tensile axis  $w$  were measured using a series of 30–40 photomicrographs taken for each specimen by SEM.

Figure 1a shows the microstructure of the FSP Al–Mg–Sc sample obtained by EBSD mapping. The black and white lines represent the HAGB (grain boundary orientation angle  $> 15^{\circ}$ ) and low angle grain boundaries (LAGB, grain boundary orientation angle  $< 15^{\circ}$ ), respectively. The microstructure was characterized by equiaxed recrystallized grains with predominantly HAGB, and the average grain size was  $\sim 0.6 \mu\text{m}$ .

Figure 1b shows the misorientation angle histogram of the FSP Al–Mg–Sc sample. The misorientation distribution is very close to the random grain assembly predicted by Mackenzie for randomly oriented cubes [30]. The average misorientation angle was  $40.3^{\circ}$ , which is very close to  $40.7^{\circ}$  for a random misorientation distribution [30]. The fraction of the HAGB was 95% and very close to 97% for a true random grain assembly [30]. Because misorientations  $< 2^{\circ}$  were not considered, the proportion of the HAGB is not a very accurate value

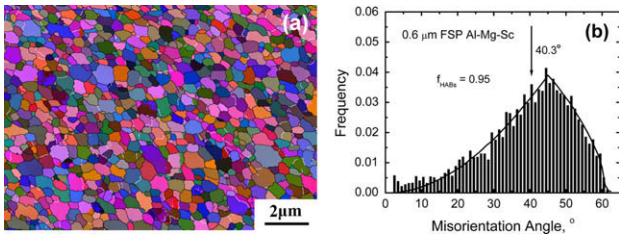


**Figure 1.** Microstructure of FSP Al–Mg–Sc alloy: (a) EBSD map; (b) boundary misorientation angle distribution (misorientations <math>< 2^\circ</math> were not considered).

[31,32]. Similarly, a high ratio of HAGB was reported in several FSP/FSW aluminum alloys [3,33]. This is attributed to the occurrence of complete dynamic recrystallization in the SZ during FSP/FSW due to intense plastic deformation at elevated temperatures.

Figure 2a shows the variation in elongation with the initial strain rate for the FSP Al–Mg–Sc. At 175 °C, the FSP Al–Mg–Sc exhibited a maximum elongation of 210%. This indicates that LTSP at 175 °C was developed in the UFG Al–Mg–Sc. When the temperature was increased from 175 to 300 °C, the optimum strain rate and maximum elongation increased from  $1 \times 10^{-4} \text{ s}^{-1}$  and 210% to  $1 \times 10^{-2} \text{ s}^{-1}$  and 560%, respectively. At 350 °C, the maximum elongation dropped to 190%. In previous reports, an elongation of 240% was obtained in UFG FSP Al–4 Mg–1Zr alloy at 175 °C [5]; this is the lowest reported temperature for LTSP of aluminum alloys. These indicate that FSP is an effective processing technique for creating UFG microstructure in aluminum alloys capable of exhibiting LTSP at temperatures  $< 0.5 T_m$ .

Figure 2b shows the variation in flow stress (at true strain of 0.1) with the initial strain rate for the FSP Al–Mg–Sc. At 175 °C, an  $m$  value of 0.33 was observed at  $1 \times 10^{-4} \text{ s}^{-1}$ . This is consistent with the observation in FSP Al–4 Mg–1Zr [5]. The strain rate sensitivity for maximum superplasticity increased to 0.5 as the temperature increased from 200 to 300 °C. At 350 °C, the  $m$  values were consistently lower than 0.3 for various strain rates. The low  $m$  values correspond to the low elongation in the FSP sample at 350 °C.

Figure 3 shows the typical offsets of marker lines on the surfaces of specimens deformed at 175 °C and  $1 \times 10^{-4} \text{ s}^{-1}$  to different elongations. The grains remained equiaxed in shape during deformation. Close inspection revealed that the marker lines were sharply defined and exhibited distinct sliding offsets at many grain boundaries. The sliding offsets tended to increase with an increase in elongation. When the specimen was pulled to an elongation of 80%, the specimen

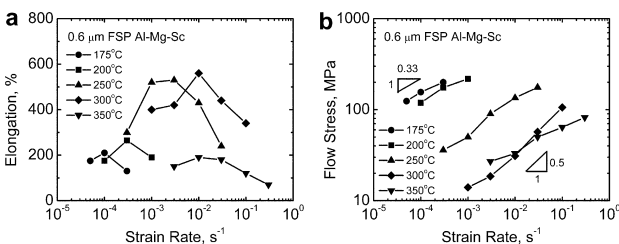


**Figure 2.** Variation in (a) elongation and (b) flow stress with initial strain rate for FSP Al–Mg–Sc alloy.

showed evidence of grain rotation and development of cavities at the grain triple junctions or the grain boundaries. Most of the cavities tended to develop perpendicular to the tensile direction. Further, the sliding directions of some grains were clearly visible, as indicated by the arrows in Figure 3c.

The GBS contributions were determined by measuring the sliding offsets ( $w$ ) combined with measurements of the mean linear intercept grain sizes ( $L$ ) [34].

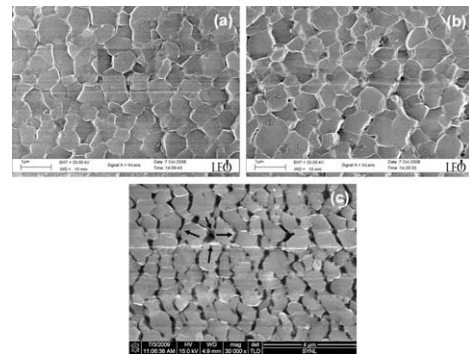
$$\epsilon_{gbs} = \phi \frac{\bar{w}}{\bar{L}} \quad (1)$$

where  $\bar{w}$  is the average value of  $w$ ,  $\bar{L}$  is the mean linear intercept grain size, and  $\phi$  is a constant with a value which was estimated both experimentally and theoretically to be  $\sim 1.5$ . If  $\epsilon_{total}$  denotes the total strain in the specimen, the contribution of GBS to the strain  $\zeta$  may be expressed as a fractional relationship [35]:

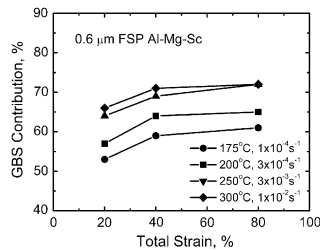
$$\zeta = \frac{\epsilon_{gbs}}{\epsilon_{total}} \quad (2)$$

Figure 4 shows the measurement results of the GBS contribution to the strain at different temperatures after testing to different strains. It is apparent that the contribution of GBS to the total strain was higher than 50% at all testing conditions. The  $\zeta$  value increased from 53% to 61% as the strain was increased from 20% to 80% at 175 °C. There is a sharp increase in the GBS contribution when the strain increased from 20% to 40% at the test temperature range. This result is consistent with the previous report [12]. However, when the strain increased from 40% to 80%, there was only a slight increase in the GBS contribution. The reason for this may be that, besides GBS, the grain rotation and cavity formation also occurred at a higher strain range as shown in Figure 3c. Furthermore, the  $\zeta$  values increased with increasing temperature and reached a maximum value of 72% at 300 °C. This is consistent with the result that higher elongation was obtained at higher temperatures.

Clearly, GBS did operate at temperatures as low as 175 °C in the UFG FSP Al–Mg–Sc, especially for the later straining stage, though the strain rate sensitivity is only  $\sim 0.33$ . The occurrence of GBS during high temperature plastic flow is closely related to the grain boundary characters [36,37]. It is generally believed that GBS occurs along the HAGB, whereas LAGB are considered



**Figure 3.** SEM micrographs showing offsets of marker lines in FSP Al–Mg–Sc alloy specimens deformed at 175 °C and  $1 \times 10^{-4} \text{ s}^{-1}$  to elongations of: (a)  $\sim 20\%$ ; (b)  $\sim 40\%$ ; (c)  $\sim 80\%$  (the loading direction is horizontal).



**Figure 4.** GBS contribution to total strain at different temperatures after testing to different strains.

immobile with respect to grain sliding [38]. The fraction of the HAGB as high as 95% in the UFG FSP Al–Mg–Sc is significantly higher than that in conventional TMT and ECAP aluminum alloys with a typical HAGB ratio of 50–65% and 60–80%, respectively [32,39–42], though a high ratio of the HAGB (~90%) with a nearly random misorientation distribution could also be achieved in aluminum alloys by TMT under a large strain of ~5.6 [43]. An exceptionally high ratio of the HAGB made GBS take place easily, and made the contribution of GBS to the total strain increase, resulting in the occurrence of superplasticity at temperatures as low as 175 °C in the UFG FSP Al–Mg–Sc with GBS as a primary superplastic deformation mechanism.

For the TMT 5083Al deformed at 250 °C, with an increase in strain from 45 to 70%, the contribution of GBS was ~27%. When the strain increased from 235% to 285%, the contribution of GBS increased to ~62% [12]. GBS contribution in the UFG FSP Al–Mg–Sc was significant higher than that in TMT 5083Al at a low strain range. This is attributed to the higher fraction of the HAGB in the UFG FSP Al–Mg–Sc.

In summary, the following conclusions were reached:

1. Fine grains 0.6 μm in size were produced in Al–Mg–Sc alloy by FSP. EBSD analyses showed that the fraction of the HAGB was 95%. The FSP Al–Mg–Sc exhibited a superplastic elongation of 210% at 175 °C and  $1 \times 10^{-4} \text{ s}^{-1}$ . A maximum elongation of 560% was obtained at 300 °C and  $1 \times 10^{-2} \text{ s}^{-1}$ .
2. Scratching marker lines using the nano-indenter is a feasible method of determining the GBS contribution to total superplastic strain for UFG materials.
3. Marker line offset measurements showed that the GBS contribution to the total strain for the UFG FSP Al–Mg–Sc exceeded 50% at 175 °C and increased with increasing strain and temperature. The occurrence of superplasticity with a high GBS contribution at 175 °C was attributed to an exceptionally high ratio of HAGB.

This work was supported by the National Natural Science Foundation of China under Grant Nos. 50671103, 50871111 and 50890171, the National Basic Research Program of China under Grant No. 2006CB605205, the National Outstanding Young Scientist Foundation under Grant No. 50525103, and the Hundred Talents Program of the Chinese Academy of Sciences.

[1] I. Charit, R.S. Mishra, *Acta Mater.* 53 (2005) 4211.

[2] H.P. Pu, F.C. Liu, J.C. Huang, *Metall. Mater. Trans. A* 26 (1995) 1153.

- [3] F.C. Liu, Z.Y. Ma, L.Q. Cheng, *Scripta Mater.* 60 (2009) 968.
- [4] F.C. Liu, Z.Y. Ma, *Scripta Mater.* 58 (2008) 667.
- [5] Z.Y. Ma, R.S. Mishra, *Scripta Mater.* 53 (2005) 75.
- [6] F. Musin, R. Kaibyshev, Y. Motohashi, G. Itoh, *Scripta Mater.* 50 (2004) 511.
- [7] K.T. Park, H.J. Lee, C.S. Lee, B.D. Ahn, H.S. Cho, D.H. Shin, *Mater. Trans.* 45 (2004) 958.
- [8] M. Noda, Hirohashi, K. Funami, *Mater. Trans.* 44 (2003) 2288.
- [9] R. Kaibyshev, T. Sakai, I. Nikulin, F. Musin, A. Goloborodko, *Mater. Sci. Technol.* 19 (2003) 1491.
- [10] K.T. Park, D.Y. Hwang, S.Y. Chang, D.H. Shin, *Metall. Mater. Trans.* 33A (2002) 2859.
- [11] S. Ota, H. Akamatsu, K. Neishi, M. Furukawa, Z. Horita, T.G. Langdon, *Mater. Trans.* 43 (2002) 2364.
- [12] I.C. Hsiao, J.C. Huang, *Metall. Mater. Trans.* 33A (2002) 1373.
- [13] R.S. Mishra, R.Z. Valiev, S.X. McFadden, R.K. Islamgaliev, A.K. Mukherjee, *Philos. Mag.* A 81 (2001) 37.
- [14] S. Komura, Z. Horita, M. Furukawa, M. Nemoto, T.G. Langdon, *Metall. Mater. Trans.* 32A (2001) 707.
- [15] N. Tsuji, K. Shiotsuki, Y. Saito, *Mater. Trans.* 40 (1999) 765.
- [16] I.C. Hsiao, J.C. Huang, *Scripta Mater.* 40 (1998) 697.
- [17] E.M. Taleff, G.A. Henshall, T.G. Nieh, D.R. Lesuer, J. Wadsworth, *Metall. Mater. Trans.* 29A (1998) 1081.
- [18] P.B. Berbon, N.K. Tsenev, R.Z. Valiev, M. Furukawa, Z. Horita, M. Nemoto, T.G. Langdon, *Metall. Mater. Trans.* 29A (1998) 2237.
- [19] R.Z. Valiev, N.K. Salimonenko, P.B. Tsenev, T.G. Berbon, T.G. Langdon, *Scripta Mater.* 37 (1997) 1945.
- [20] H.P. Pu, F.C. Liu, J.C. Huang, *Metall. Mater. Trans.* 26A (1995) 1153.
- [21] T.R. McNelley, R. Crooks, P.N. Kalu, S.A. Rogers, *Mater. Sci. Eng. A* 106 (1993) 135.
- [22] R.Z. Valiev, A.V. Korznikov, R.R. Mulyukov, *Mater. Sci. Eng. A* 168 (1993) 141.
- [23] T.R. McNelley, E.W. Lee, M.E. Mills, *Metall. Trans.* 17A (1986) 1035.
- [24] W.M. Thomas, E.D. Nicholas, J.C. Needham, M.G. Murch, P. Templesmith, C.J. Dawes, G.B. Patent Application No. 9125978.8, December 1991.
- [25] R.S. Mishra, Z.Y. Ma, *Mater. Sci. Eng. R50* (2005) 1.
- [26] R.B. Vastava, T.G. Langdon, *Acta Metall.* 27 (1979) 251.
- [27] T.G. Langdon, *J. Mater. Sci.* 16 (1981) 2613.
- [28] P. Shariat, R.B. Vastava, T.G. Langdon, *Acta Metall.* 30 (1982) 285.
- [29] Z.R. Lin, A.H. Chokshi, T.G. Langdon, *J. Mater. Sci.* 23 (1998) 2712.
- [30] J.K. Mackenzie, *Biometrika* 45 (1958) 229.
- [31] O.V. Mishin, A. Godfrey, L. Östensson, *Metall. Trans.* 37A (2006) 489.
- [32] O.V. Mishin, D. Juul Jensen, N. Hansen, *Mater. Sci. Eng. A* 342 (2003) 320.
- [33] A.P. Gerlich, T. Shibayanagi, *Scripta Mater.* 60 (2009) 239.
- [34] T.G. Langdon, *Metall. Trans.* 3 (1972) 797.
- [35] T.G. Langdon, *J. Mater. Sci.* 41 (2006) 597–609.
- [36] T. Watanabe, *Mater. Sci. Eng. A* 166 (1993) 11.
- [37] M. Kawasaki, T.G. Langdon, *Mater. Trans.* 49 (2008) 84.
- [38] H. Kokawa, T. Watanabe, S. Karashima, *Philos. Mag. A* 44 (1981) 1239.
- [39] R. Kaibyshev, E. Avtokratova, A. Apollonov, R. Davies, *Scripta Mater.* 54 (2006) 2119.
- [40] T.R. McNelley, M.E. McMahon, *Metall. Mater. Trans.* 28A (1997) 1879.
- [41] M. Eddahbi, T.R. McNelley, O.A. Ruano, *Metall. Mater. Trans.* 32A (2001) 1093.
- [42] M. Ferry, N.E. Hamilton, F.J. Humphreys, *Acta Mater.* 53 (2005) 1097.
- [43] J.C. Huang, I.C. Hsiao, T.D. Wang, B.Y. Lo, *Scripta Mater.* 43 (2000) 213.